Fumaroles in ice caves on the summit of Mount Rainier— preliminary stable isotope, gas, and geochemical studies

D.R. Zimbelman[a,*], R.O. Rye[b], G.P. Landis[b]

[a]US National Park Service, Mount Rainier National Park, Tahoma Star Woods Route, Ashford, WA 98304, USA
[b]US Geological Survey, P.O. Box 25046, Mail Stop 963, Denver, CO 80225, USA

Abstract

The edifice of Mount Rainier, an active stratovolcano, has episodically collapsed leading to major debris flows. The largest debris flows are related to argillically altered rock which leave areas of the edifice prone to failure. The argillic alteration results from the neutralization of acidic magmatic gases that condense in a meteoric water hydrothermal system fed by the melting of a thick mantle of glacial ice. Two craters atop a 2000-year-old cone on the summit of the volcano contain the world's largest volcanic ice-cave system. In the spring of 1997 two active fumaroles ($T = 62°C$) in the caves were sampled for stable isotopic, gas, and geochemical studies.

Stable isotope data on fumarole condensates show significant excess deuterium with calculated δD and $\delta^{18}O$ values (-234 and $-33.2‰$, respectively) for the vapor that are consistent with an origin as secondary steam from a shallow water table which has been heated by underlying magmatic–hydrothermal steam. Between 1982 and 1997, δD of the fumarole vapor may have decreased by 30‰.

The compositions of fumarole gases vary in time and space but typically consist of air components slightly modified by their solubilities in water and additions of CO_2 and CH_4. The elevated CO_2 contents ($\delta^{13}C_{CO_2} = -11.8 \pm 0.7‰$), with spikes of over 10,000 ppm, require the episodic addition of magmatic components into the underlying hydrothermal system. Although only traces of H_2S were detected in the fumaroles, most notably in a sample which had an air $\delta^{13}C_{CO_2}$ signature ($-8.8‰$), incrustations around a dormant vent containing small amounts of acid sulfate minerals (natroalunite, minamiite, and wood-houseite) indicate higher H_2S (or possibly SO_2) concentrations in past fumarolic gases.

Condensate samples from fumaroles are very dilute, slightly acidic, and enriched in elements observed in the much higher temperature fumaroles at Mount St. Helens (K and Na up to the ppm level; metals such as Al, Pb, Zn Fe and Mn up to the ppb level and volatiles such as Cl, S, and F up to the ppb level).

The data indicate that the hydrothermal system in the edifice at Mount Rainier consists of meteoric water reservoirs, which receive gas and steam from an underlying magmatic system. At present the magmatic system is largely flooded by the meteoric water system. However, magmatic components have episodically vented at the surface as witnessed by the mineralogy of incrustations around inactive vents and gas compositions in the active fumaroles. The composition of fumarole gases during magmatic degassing is distinct and, if sustained, could be lethal. The extent to which hydrothermal alteration is currently occurring at depth, and its possible influence on future edifice collapse, may be determined with the aid of on site analyses of fumarole gases and seismic monitoring in the ice caves. © 2000 Elsevier Science B.V. All rights reserved.

Keywords: fumaroles; magmatic; hydrothermal

* Corresponding author. Present address: G.O. Logic; P.O. Box 1878, White Salmon, WA 98672-1878, USA, +1-509-493-9269.
E-mail address: hazard@gorge.net (D.R. Zimbelman).

1. Introduction

The International Association of Volcanology and Chemistry of the Earth's Interior nominated 15 volcanoes as Decade Volcano Demonstration Projects in conjunction with the United Nations International Decade for Natural Disaster Reduction (UN Resolution 42/169/1987). The objective is to mitigate volcanic hazards. Mount Rainier, one of about two dozen recently active volcanic centers in the Cascade Range of western United States and Canada (Fig. 1), is the only Decade Volcano in North America. A science plan for the study of Mount Rainier as a Decade Volcano Demonstration Project was issued by the US National Research Council (1994). Debris flows

and debris avalanches from Mount Rainier constitute the greatest volcanic hazard in the Cascade Range (National Research Council, 1994; Hoblitt et al., 1995) and are the primary reason Mount Rainier was designated a Decade Volcano. During the Holocene, debris flows from Mount Rainier repeatedly inundated areas that are now heavily populated and experiencing rapid growth.

Recent studies at Mount Rainier document the widespread occurrence of altered rock (Zimbelman, 1996; Zimbelman and Rye, 1996; Crowley and Zimbelman, 1997) and demonstrate the importance of magmatic–hydrothermal and steam-heated systems (Rye et al., 1992; Rye, 1993) to the generation of the altered rocks. Hydrothermal alteration at Mount Rainier
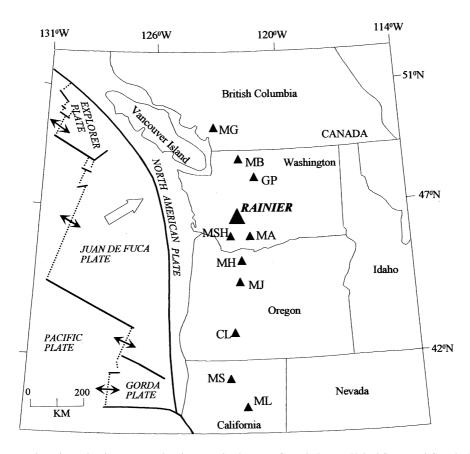

Fig. 1. Active or recently active volcanic centers and major tectonic elements, Cascade Range, United States and Canada. Triangles, major Quaternary volcanic centers: MG, Mount Garibaldi; MB, Mount Baker; GP, Glacier Peak; RAINIER, Mount Rainier; MSH, Mount St. Helens; MA, Mount Adams; MH, Mount Hood; MJ, Mount Jefferson; CL, Crater Lake; MS, Mount Shasta; ML, Lassen Peak. Solid arrows, directions of ridge-spreading; open arrow, direction of convergence of Juan de Fuca and North American plates. Tectonic elements generalized from Riddihough (1984).
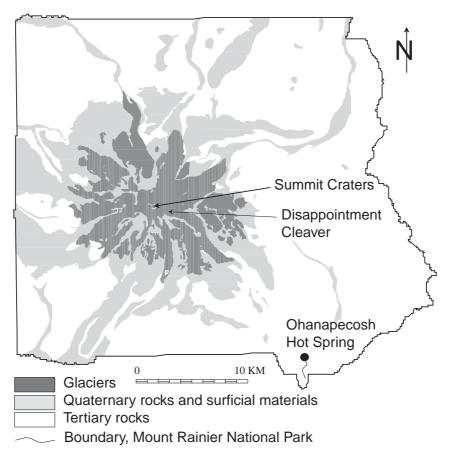
Fig. 2. Generalized distribution of Tertiary bedrock, Quaternary rock and surficial deposits, and glaciers, Mount Rainier National Park.

resulted in the formation of smectite and kaolin group clays, various forms of silica, including quartz, tridymite, cristobalite, opal, and amorphous silica, and various Al-, Ca-, Fe-, K-, Na-, and Ba-sulfates and phosphates (Zimbelman, 1996). At the summit, the sulfate minerals include alunite/natroalunite, alunogen, metaalunogen, anhydrite, and gypsum. Altered rocks on the upper flanks (ca. 3650–4200 m) characteristically include the sulfates alunite/natroalunite, gypsum, and anhydrite with lesser amounts of jarosite/natrojarosite. In contrast, lower flank altered areas typically includes assemblages where jarosite/natrojarosite is the predominant sulfate phase.

The importance of hydrothermally altered rock to volcanic landslide hazards at Mount Rainier was noted by the National Research Council (1994). Hydrothermally altered rock plays two critical roles in the generation and evolution of debris flows: (1) hydrothermally altered rock form structurally weakened zones, along which edifice collapse is likely to occur (Lopez and Williams, 1993; Zimbelman, 1996); (2) hydrothermal clay minerals are critical components to the formation of the largest and most far-reaching type of debris flows (Crandell, 1971; Scott et al., 1995).

This study is the first attempt to determine the extent to which hydrothermal alteration is presently occurring inside Mount Rainier as part of a scientifically defensible effort to assess and mitigate landslide hazard potential related to hydrothermal alteration. In the spring of 1997, a team of 15 people camped at Ingraham Flats (elev. 3353 m) and mapped and sampled fumaroles in the summit ice caves, which are frequently used by mountain climbers for shelter. This team included researchers from the US National Park Service (David Zimbelman), US Geological Survey (Jim Crowley), University of Nevada, Reno
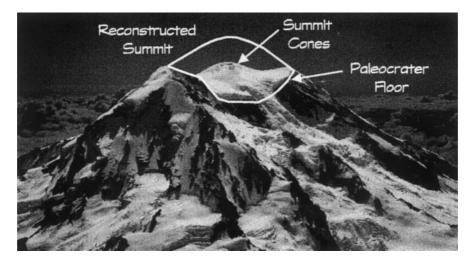
Fig. 3. Reconstructed summit, paleocrater erosion surface, and young (ca. 2200 years) summit cone at Mount Rainier volcano.

(Bob Watters, Dave Sullivan, Steve Bowman), CEA, France (Faivee Pierret), and CFR, France (Francois Le Guern) as well as French journalists and a press crew who documented the scientific endeavor. Weather and logistical conditions on the summit greatly limited the number of samples that could be obtained. This study presents chemical and isotopic data from the reconnaissance sampling of fumarole gases and condensates, ice cave melt waters, and incrustations around a dormant vent on the summit of Mount Rainier. These data are used to present constraints on the nature of the currently active hydrothermal system in the edifice of Mount Rainier.

2. Geologic setting

Among Cascade volcanoes (Fig. 1), Mount Rainier contains the most water (about 4.4 km^3), mostly as snow and ice (Driedger and Kennard, 1986), is the highest (4392 m), the third most voluminous (Sherrod and Smith, 1990), and the second most seismically active (Moran et al., 1995). Crandell (1976) determined that at least 94 km^2 of the volcano is covered by glaciers (Fig. 2). Numerous workers, including Russel (1898), Matthes (1914), Coombs (1936), Crandell (1963), Fiske et al. (1963), and Dragovich et al. (1994) noted that Mount Rainier must have been much higher in the past. Projected dips of volcanic units in areas such as Tahoma Cleaver, Little Tahoma Peak, Russell Cliff, and

Gibraltar Rock suggest a former summit height of somewhere between 4570 and 4880 m (Fig. 3). This former summit material was transformed into the Osceola Mudflow following a collapse event about 5600 years ago (Crandell and Mullineaux, 1967; Dragovich et al., 1994). Dragovich et al. (1994) calculated that the Osceola Mudflow deposit covered an area of at least 505 km^2 and had a volume of at least 3.8 km^3. Numerous other Holocene mud flows that originated on Mount Rainier (Crandell, 1963;1971; Yamaguchi, 1983) have been documented and catastrophic collapse appears to be a normal destructional process at the volcano.

The summit cone represents the climax to an 2.2 ka eruptive period that produced a widespread tephra layer (e.g. Crandell, 1976; Venezky and Rutherford, 1997). The cone is at least 300 m high, 2 km wide, and consists of two overlapping craters (Fig. 4). Both craters, ca. 500 m in diameter, are snow-free along their rims and flanks, contain caves beneath their central ice caps, and have been extensively altered during the past 2.2 ka.

3. Summit ice caves

An active hydrothermal system at Mount Rainier has been invoked as a possible explanation for a low-seismicity zone that occurs at 1–14 km depth beneath the volcano (Moran and Malone, 1997). Using aerial infrared radiometer surveys, Moxham et al. (1965), Lange
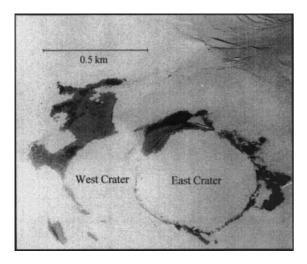
Fig. 4. Aerial photograph of Mount Rainier's summit showing west and east craters and snow-free zones.

and Avent (1975), Frank (1985), and Frank and Realmuto (1995) found thermal anomalies associated with the summit cone, extending down the west flank, and covering an area of more than 12,000 m^2 at the summit. This area hosts slightly acidic fumaroles with temperatures near the boiling point (87°C at 4392 m). The presence of

a large mantle of ice above this active hydrothermal system has resulted in the development of the world's largest known volcanic crater ice-cave system (Lokey et al., 1972; Kiver and Steele, 1975). Only a few other active volcanoes host ice caves including Mount Baker, Washington, Mount Wrangell, Alaska, and Mount Erebus, Antarctica. The caves at Mount Rainier occur along the contact between the ice and the crater floors. During numerous trips to the summit, it has been observed that the entrance passages periodically close, possibly due to plastic flowage of the ice cap into the crater. Kiver and Steele (1975) noted an increase in tunnel size from 1970 to 1973. Such changes in tunnel and entrance sizes probably reflect complex relationships between various meteorological and volcanic parameters.

The east crater has a more extensive ice-cave system than the west crater (Fig. 5). Caves in the east crater contain numerous fumaroles within a relatively large tunnel system. The tunnel system contains numerous entrances at the surface, extends as deep as 152 m (Kiver and Mumma, 1971), and can be followed, mostly within an arcuate passageway, for more than 1500 m. Generally, the tunnels form at the ice–rock contact and are steam-filled from the fumaroles. During extended
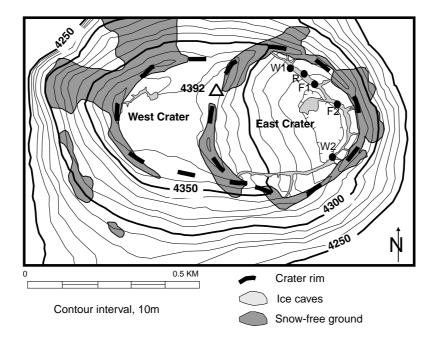

Fig. 5. Topographic map of summit craters showing approximate locations of snow-free zones and ice-cave systems.

field studies between 1993 and 1997, it was observed that cold air descends through some of the cave openings while other openings expel warm moist air. Although no body of standing water occurs in the east crater, as first noted by Flett (1912), small streams of water, derived from dripping walls and ceilings, drain through the rubble floor of the caves.

Access to the west crater is more restricted, and the tunnels are much less developed than in the east crater. This cave system, however, hosts a small crater lake (e.g. Lokey, 1973; Kiver and Steele, 1975). With a temperature of 0.5°C (Lokey, 1973), this lake is significantly warmer than ice at the volcano, which has been reported to be at subfreezing temperatures, between −4 and −10°C (Miller, 1970; Kiver and Steele, 1972). Kiver and Steele (1975) noted that the lake was sealed at the bottom by a horizon of hydrothermal clays. Only the west crater has a hydrogen sulfide odor.

Kiver and Mumma (1971) and Kiver and Steele (1972) determined that the summit ice caves ablate about 2–3 m/year, have a maximum ice thickness on the order of 120 m (east crater) and 48 m (west crater), and that the ice is replaced about once every 15 to 80 years. The caves form by the melting, from the bottom of the caves, of the ice and snow that has accumulated within the craters. Because the caves act as condensers, traps, and calorimeters for magmatic volatiles and heat (e.g. like crater lakes; Kusakabe, 1997), their characterization and monitoring may represent powerful potential indicators of changes in the hydrovolcanic system which may not be readily apparent by surface surveys.

As noted by Frank (1995), areas other than the summit of Mount Rainier that contain active geothermal manifestations include: (1) Disappointment Cleaver, which contains a small area (ca. 500 m^2) of heated ground, fumaroles with temperatures of about 55–60°C, and disseminated smectite and incrustations of poorly crystalline silica minerals; (2) several thermal springs on the lower flanks of the volcano, including areas adjacent to the Winthrop and Paradise glaciers, which generally have temperatures below 25°C, are enriched in sulfate and carbon dioxide, and have precipitated calcite, opal, and gypsum (e.g. Nehring et al., 1979; Mariner et al., 1993); and (3) travertine mounds at Ohanapecosh hot springs (40–48°C) at the base of Mount Rainier.

4. Methods

The gas samples were collected in evacuated 300 cm^3 glass containers with a single teflon stopcock. Eleven samples of gas from fumaroles ($T = 62$°C) in the east crater cave were collected, 5 on May 19, 1997 and 6 on June 7, 1997. Samples collected on May 19 include 2 from the upper fumarole and 3 from the lower fumarole; samples collected on June 7 include 4 from the upper fumarole and 2 from the lower fumarole (Fig. 5). Condensates were collected by allowing fumarolic vapor to condense into a wide mouth 1 l bottle and transferring the condensed water numerous times to a smaller container until enough sample was accumulated. Two samples of melt water were also obtained at locations 500 m apart in the cave. Incrustations from fumarole vents in the west crater were collected for mineralogic analysis.

Fumarole gas components were analyzed by removing a small (1 cc) aliquot of gas from each of the 300 cc sample flasks and injecting it into the inlet manifold of a quadrupole mass spectrometer (QMS). The QMS previously was calibrated using a certified "air" reference gas and secondary standards. QMS analytical methods enable rapid ppm-level analysis of gases from extremely small samples ($\leq 10^{-15}$ mol of CO_2 in air). Details of analytical methods are reported in Landis and Hofstra (1991) and Landis et al. (1995).

Fumarole gas samples were analyzed for N_2, O_2, Ar, CO_2, and CH_4, and $\delta^{13}C_{CO_2}$, and mass spectra from AMU (m/e) = 1–160 were inspected for additional gas species. Low ppm levels of H_2S were noted in several samples, but SO_2 was not. All mass intensities were adequately accounted for by the specified gas species and no other gases were detected.

For measurement of carbon isotope analyses of CO_2 approximately half of the sample flask gas mixture was removed and CO_2 cryogenically separated and purified, placed in capillary break seals, and the $\delta^{13}C$ determined by conventional gas ratio mass spectrometry. Data are reported as per mil values relative to PDB standard. Hydrogen and oxygen isotope composition of fumarole condensates and melt water were determined by conventional methods and reported relative to SMOW.

Chemical composition of fumarole condensates were determined by ICP-AES and IC methods and

the mineralogy of incrustations around dormant fumaroles were determined by XRD.

5. Results

Stable isotope data for fumarole condensates, calculated vapor compositions, melt water, and carbonates from travertine deposited on the flank and base of the volcano are presented in Table 1. Hydrogen and oxygen isotope data are plotted in Fig. 6. The carbonate isotope data are included for comparison with isotope data on CO_2 in the gas samples. Fumarole gas compositions are reported as volume (mole) percent and ppmV (by volume) for major and minor species, respectively, in Table 2 along with data on gas ratios, gas solubility in water and gas composition of air in the caves and $\delta^{13}C$ data on CO_2. The gas data are plotted in Figs. 7 and 8. Chemical data for the fumarole condensates and melt water in the east crater ice caves are summarized in Table 3.

6. Stable isotope geochemistry

6.1. Isotopic composition of melt water in the east crater cave

Any stable isotope study of a hydrothermal system requires the determination of the composition of ambient meteoric water that may serve as a source of recharge to the system. The δD values of melt water from two locations are −148 and −150‰ (Table 1). These water samples were presumably derived from the melting of glacial ice by heat from the fumaroles, as part of the process, which sustains the caves. Since the samples were collected several hundred meters apart in a large cave which is as much as 150 m deep we anticipated that the isotope data would represent an average value for the composition of a considerable section of the bottom of the glacier and thus serve as an average value for possible recharge to the fumaroles. However, the δD values for melt water are much less negative than the −190‰ value obtained by Frank (1985, 1995) for firn collected outside of the caves in 1982. On the basis of very limited sampling Frank also determined that higher altitude samples of firn show a $\delta^{18}O$ and

δD variation of about −9 and −65‰/km, respectively. This δD variation is comparable with −50/km for snow and firn at high elevations at Blue Glacier, WA (Sharp et al., 1960).

It has long been recognized that the isotopic composition of precipitation at a given elevation depends largely on the annual mean temperature which can vary considerably during individual storms, from storm to storm in a given season with large seasonal differences between summer and winter (Sharp et al., 1960; Dansgaard, 1964; Deutsch et al., 1966). Thus, the isotopic composition of the firn reflects the annual mean temperature of precipitation of snow with modification by additions of melt water and rain that percolates into the firn. Prior to collection of the samples in May 1997, very large amounts of wet snow and rain accumulated on the summit of Mount Rainier. The ceiling to the snow caves is quite porous and the heavy isotopic composition obtained for our melt water samples almost certainly reflects modification of the composition of firn melt in the summit caves by incorporation of recent rain water. Until more studies are done the best average isotope values for firn on the summit are those ($\delta D = -190$ and $\delta^{18}O = -4.6‰$) obtained by Frank (1985,1995).

6.2. Isotopic composition of fumarole vapor and condensates in the east crater cave

The δD and $\delta^{18}O$ values for the upper and lower fumarole condensates are nearly identical at −188 ± 1 and −26 ± 0.2‰, respectively (Table 1). The isotopic composition of fumaroles condensates collected in containers open to air must be corrected for isotopic fractionation that occurs during condensation. The temperature of the fumaroles was 62°C. Using the fractionation factors for O and H between water and vapor at 62°C as summarized in O'Neil and Friedman (1977) the average δD and $\delta^{18}O$ values of the vapor prior to condensation is calculated to average −234 and −33.2‰, respectively. The isotope values for the vapor collected at the surface must be modeled in terms of the isotope composition of water from which the vapor was derived at depth. The isotopic composition of the vapor collected at the surface is determined by the thermal, mixing and steam separation history of the underlying water (Truesdell et al., 1977; Giggenbach and Stewart, 1982). At this time we

Table 1

Stable isotope data for firn melt, fumarole condensate and calculated vapor, travertine and calculated travertine fluids

Sample	Location	Elevation (m)	T (°C)	δD_{H_2O}	$\delta^{18}O_{H_2O}$	$\delta^{13}Ccc$	$\delta^{13}C_{CO_2}$[a]	$\delta^{18}Occ$	$\delta^{18}O_{H_2O}$[a]
Firn melt	East Crater near entrance	4390	2	−150	−20.4				
Firn melt	East Crater 500 m from entrance	4390	2	−148	−20.4				
Condensate	East Crater snow cave upper fumarole	4390	62	−187	−26.8				
Condensate	East Crater snow cave lower fumarole	4390	62	−189	−27.3				
Vapor[a]	East Crater snow cave upper fumarole	4390	62	−234	−33.2				
Vapor[a]	East Crater snow cave lower fumarole	4390	62	−236	−33.7				
Travertine	Disappointment Cleaver fumarole area	3745	60			−5.2	−12.3	3.4	−18.8
Travertine	Ohanapecosh Hot Spring	620	40			−7.2	−16.2	11	−14

[a] Calculated.

do not have enough information to model the isotopic composition of the underlying water. As shown in Fig. 6 the isotopic composition for the vapor contains excess deuterium and lies well to the left of the meteoric water line. Furthermore, the isotopic composition of vapor collected from the fumaroles in the ice caves is considerably lower in D and ^{18}O than that for the presumed value for firn on the summit. As pointed out by Frank (1985,1995) and as shown schematically in Fig. 6 such isotope depletions in fumarolic vapor is consistent with vapor which originates as secondary steam from a shallow water table which has been heated by underlying primary steam (Giggenbach and Stewart, 1982).

In 1982, Frank measured δD and $\delta^{18}O$ values −162 ± 1 and −23 ± 0.2‰, respectively, for condensate collected from a fumarole at the summit. Using temperatures of 72°C he calculated values of $\delta D = -203$ and $\delta^{18}O = -29.6$ for the vapor. The δD values obtained by Frank (1985) are close to those of the presumed composition ($\delta D = -190$) for firn on the summit. Our data when compared to those of Frank (1985) indicate a change of nearly 30‰ in the δD of the fumarole vapor from 1982 to 1997. This change needs to be verified by closed system collections of condensate that do not permit the possibility of liquid/vapor isotope fractionation during sampling. However the change is probably too large to be an artifact of the sampling method. It is also too large

to be due to change in the *average* composition of precipitation. Arehart et al. (1995) also noted distinct temporal changes in isotopic characteristics in fumarole condensates at Galeras volcano, Colombia.

Shallow hydrothermal systems that involve one or more cycles of secondary steam can be complex and the cause of the shift in δD of the fumarolic vapor is not known. The important point is that monitoring of the isotopic composition of the vapor may permit detection of significant changes in the nature of the fluid vapor system at depth.

6.3. Isotopic composition of travertine on Mount Rainier

Isotopic data from travertine collected near fumaroles at Disappointment Cleaver (3745 m), on the flank of the volcano, and Ohanapecosh hot spring (620 m), at the base of the volcano, are summarized in Table 1. The calculated $\delta^{13}C$ values of CO_2 and $\delta^{18}O$ values of H_2O in equilibrium with the travertine at the presumed temperatures of deposition are also presented. These data provide a framework for interpretation of $\delta^{13}C$ data on CO_2 from the fumaroles at the summit. Travertine deposition occurs due to the loss of CO_2 as liquid hydrothermal solutions vent at the surface. Travertine deposition does not occur from vapor phase fumaroles. The temperatures of travertine deposition at Disappointment Cleaver were measured
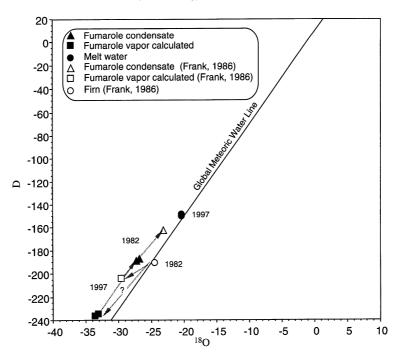
Fig. 6. H and O isotope plot of condensates, calculated vapor, and melt water for this study and for samples collected in 1982 by Frank (1985). Arrows show possible evolution of water compositions from secondary steam in a shallow water table which has been heated by underlying primary steam (Giggenbach and Stewart, 1982).

by Frank (1985) at 55–60°C. The solutions in the hot springs at Ohanapecosh had a temperature of 40°C at the time the travertine was collected. The calculated $\delta^{13}C_{CO_2}$ value for travertine fluids at 60°C at Disappointment Cleaver is −12.3‰ and is within the range obtained in this study for CO_2 from fumaroles at the summit. The $\delta^{13}C_{CO2}$ value for calcite at Ohanapecosh is −16.2‰. The low $\delta^{13}C$ value is probably derived from organic matter that enters the volcano in meteoric water recharge at the lower elevations of the heavily forested mountain. The calculated $\delta^{18}O$ values for water in equilibrium with the travertine are −16.8‰ at Disappointment Cleaver and −14‰ at Ohanapecosh Hot Spring. These values reflect the latitude dependence on the isotopic composition of meteoric water as observed by Frank (1985).

7. Gas geochemistry

The fumarole gas data presented in Table 2 contain N_2, O_2, Ar, CO_2, and CH_4, and only trace amounts of

H_2S. The ambient air samples from the ice caves have typical air gas compositions (N_2 = 79%, O_2 = 20%, CO_2 = 365 ppm Ar = 9200 ppm, CH_4 = 1.13 ppm) except for a trace of H_2S. Except for three samples, discussed below, summit fumarole gas compositions vary over a narrow range with median values of N_2 = 76.2%; O_2 = 22.4%; Ar = 9068 ppm; CO_2 = 4009 ppm; CH_4 = 1.82 ppm. Except for two samples, fumarole gases from the summit of Mount Rainier have CO_2 enrichments of 7 to nearly 30 times that of air. Elevated CO_2 contents were also observed by Frank (1985, 1995) using GC methods. Thus, most samples contain the major air components, but are somewhat depleted in nitrogen and argon, elevated in oxygen and methane, greatly enriched in carbon dioxide, and two samples have traces of H_2S. Interestingly, the two samples (MR011 and MR021) with the lowest (air-like) CO_2 contents are the ones with trace H_2S. Sample MR004 is clearly anomalous. It has CO_2 and CH_4 in excess of 10,000 ppm and 4.5 ppm, respectively, high concentrations of nitrogen (96.4%) and argon (11900 ppm) and low oxygen

Table 2
Mount Rainier summit gas data[a]

Sample#	N$_2$ (mol%)	O$_2$ (mol%)	Ar (ppm)	CO$_2$ (ppm)	CH$_4$ (ppm)	H$_2$S	δ^{13}C of CO$_2$	CO$_2$/CH$_4$	N$_2$/Ar	N$_2$/CO$_2$	O$_2$/Ar	N$_2$/Ar (R/R$_a$)	O$_2$/Ar (R/R$_a$)	N$_2$/CO$_2$ (R/R$_a$)	N$_2$/(O$_2$ + Ar)
Air samples															
MR001	79.0744	19.9660	9234	361	1.16			311.21	85.63	2190	21.62	1.024	0.964	1.00988	3.78538
MR002	78.5973	20.4450	9211	365	1.13	det.		323.01	85.33	2153	22.20	1.021	0.990	0.99278	3.67860
MR003	78.4658	20.5775	9188	378	1.13	det.		334.51	85.40	2076	22.40	1.022	0.998	0.95704	3.65020
May 19 samples															
MR004	96.3925	1.3783	11928	10359	4.59		−11.72	2256.86	80.81	93	1.16	0.967	0.052	0.04290	37.49076
MR005	75.8583	22.7944	9068	4404	1.67		−12.47	2637.13	83.65	172	25.14	1.001	1.121	0.07941	3.20061
MR009	76.1947	22.4598	9148	4306	1.84		−12.38	2340.22	83.29	177	24.55	0.996	1.095	0.08158	3.25972
MR011	76.4567	22.6133	8960	339	1.01	det.	−8.83	335.64	85.33	2255	25.24	1.021	1.125	1.03982	3.25219
MR013	76.2282	22.3803	9209	4703	2.07		−12.47	2271.98	82.78	162	24.30	0.990	1.083	0.07473	3.27143
June 7 samples															
MR015	76.6141	22.2445	8969	2443	1.50		−12.47	1628.67	85.42	314	24.80	1.022	1.106	0.14459	3.31069
MR017	76.6202	22.0731	9057	4009	1.82		−12.28	2202.75	84.60	191	24.37	1.012	1.087	0.08811	3.33439
MR019	76.6343	21.9976	9217	4462	1.86		−12.00	2398.92	83.14	172	23.87	0.995	1.064	0.07918	3.34366
MR021	76.4159	22.6181	8857	803	1.14	det.	−11.08	704.39	86.28	952	25.54	1.032	1.139	0.43874	3.25121
MR022	76.2075	22.4935	9053	3936	1.75		−11.89	2249.14	84.18	194	24.85	1.007	1.108	0.08927	3.25690
MR025	76.1954	22.5249	8913	3882	1.89		−12.37	2053.97	85.49	196	25.27	1.023	1.127	0.09049	3.25396
Summit average	76.2282	22.3803	9068	4009	1.82		−12.37	2249.14	83.29	172	24.30	0.996	1.083	0.07941	3.27143
Solubility data															
Air	78.0840	20.9460	9340	360	1.60		−8.50	225.00	83.60	2169	22.43	1.000	1.000	1.00000	3.56874
AirSol25									38.98	42	20.48	0.466	0.913	0.01919	
AirSolr60									43.50	64	21.03	0.520	0.938	0.02951	
PureSol25									0.47	0.	0.91	0.006	0.041	0.00001	
PureSol60									0.52	0.	0.94	0.006	0.042	0.00001	

[a] Note: data are in mole percent and ppmV, det. indicates presence of hydrogen sulfide as detected at mass 34 after correction for oxygen, and R indicates ratio of sample and R_a that of atmosphere. Summit average data are calculated from samples exclusive of air and magmatic pulse. AirSol25 and AirSol60 are the atmospheric gas solubility in water at 25 and 60°C for comparison with air values. PureSol data are for pure gas STP. Lines between rows for each sampling day separate upper fumarole from lower fumarole samples (both at 62°C vent temperature).
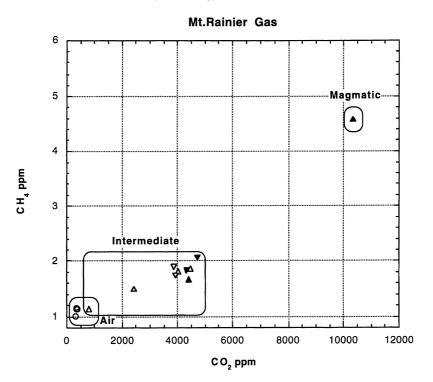
Mt. Rainier Gas

Fig. 7. Plot of methane versus carbon dioxide with solid symbols representing May 19 data and open symbols representing June 7 data. Upper and lower fumaroles are respectively up and down pointing triangles. Though dominantly atmospheric in composition, the fumarole gases are shifted toward a composition.

(1.4%) contents relative to the other samples. A gas flux of this composition would be lethal if sustained long enough to affect the composition of air in the ice caves.

The fumarole gas compositions are highly variable in time and space (Table 2). Methane concentrations correlate with carbon dioxide (Fig. 7) with large variability in samples collected on different days (May 19 or June 7), from different locations (upper and lower fumarole), and over the few minutes required to collect replicate samples at a single fumarole on the same day. Three groups of gas compositions are recognized in Fig. 7, an air gas composition with CO_2 near 365 ppm, a dominantly air gas composition but with intermediate CO_2 averaging approximately 4000 ppm, and a non air gas composition with a CO_2 concentration $>10,000$ ppm.

The $\delta^{13}C$ of the CO_2 in the atmosphere in the caves was not measured, but the value of present day atmospheric CO_2 is typically $-7‰$ (Faure, 1986). The CO_2 in most of the gas samples have a narrow range of low

$\delta^{13}C$ values with an average of $-12.4‰$. The sample (MR011) with the lowest CO_2 and CH_4 contents has a $\delta^{13}C$ value ($-8.8‰$) close to that of atmospheric CO_2.

The CO_2 concentration of $>10,000$ ppm for sample MR004 is similar to the concentration spikes recently monitored for fumaroles occurring in a labyrinth of ice caves on Mount Erebus, an ice-capped active volcano in Antarctica (Philip Kyle, pers. commun., 1998). Though the fumarolic gases on Mount Rainier consist largely of air gas species, they clearly contain magmatic contributions as supported by the $\delta^{13}C$ values of the CO_2. The sample with the highest CO_2 and CH_4 content (MR004) has a $\delta^{13}C_{CO2}$ value of $-11.7‰$ as compared to the median value of $-12.4‰$ for most of the fumaroles. The difference may reflect the variability in the $\delta^{13}C$ of deep seated carbon. However the variation may also reflect a small carbon isotope fractionation (Grootes et al., 1969) during phase separation and/or condensation in the hydrothermal system. The carbon isotope composition of the highest CO_2 sample (MR004) is similar
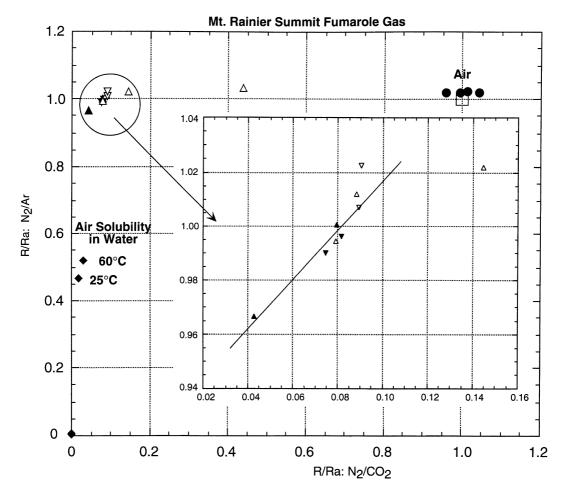
Fig. 8. R/R_a of N_2/Ar versus N_2/CO_2 where R is ratio of gases in a sample and R_a is ratio of the gases in air. Air would therefore have a $R/R_a = 1$. Air solubility ratios for solution and phase separation at both 25 and 60°C are plotted for reference, as well as absolute gas solubility data for pure gases. Unlike atmospheric samples, summit fumaroles plot well-removed from these values and clearly indicate a magmatic component of carbon dioxide in "air-like" nitrogen/argon. The insert shows a systematic variation between N_2/Ar and N_2/CO_2 that is unlike that predicted from the temperature dependent solubility of these gases in water. Symbols are the same as in Fig. 7.

to that obtained for magmatic CO_2 from Mount St. Helens after the 1980 eruption (-11.5‰; Evans et al., 1981) and is probably typical of magmatic CO_2 for Mount Rainier. This low value for magmatic CO_2, as opposed to the typical value of -7.5 ± 0.5‰ for deep seated carbon (Javoy et al., 1986) probably reflects the importance of a subducted organic matter component to the deep carbon reservoir beneath Mt. Rainier.

Most of the summit vent gases clearly are dominated by atmospheric components. For example, the average $N_2/(O_2 + Ar)$ of the fumaroles is 3.27

compared to 3.57 for air (Table 2). Yet the fumarole gases are not simply air that has been dissolved into hydrothermal fluids and then released during phase separation. Fig. 8 is a plot of R/R_a for N_2/Ar versus N_2/CO_2, where R is the ratio in the sample and R_a is that in the atmosphere. In this plot air has a $R/R_a = 1$. The compositions predicted for air gases if they are dissolved in water at 25 and 60°C and later released by phase separation are plotted for reference. The fumarole gases at Mount Rainier cannot be derived by this means, even at elevated pressures and temperatures.

Though N_2/Ar is not much different from air (83.6

or near 1.0 as R/R_a in Fig. 8), the low N_2/CO_2 indicates large enrichment in CO_2. Fig. 8 demonstrates that fumarole gases consist of air entrained in fumarole vapor with a significant addition of magmatic CO_2. The insert in Fig. 8 shows a systematic variation in the gas ratios for fumarole samples similar to that illustrated in Fig. 7. The trend reflects variable contributions of magmatic CO_2 with minor solubility-controlled variation in argon content. The entrainment of air will promote oxidation of sulfur species and result in the formation of steam-heated acid-sulfate alteration mineral assemblages characterized by the minerals alunite and/or jarosite (Rye et al., 1989, 1992; Stoffregen, 1993; Zimbelman and Rye 1996).

The absence of other magmatic volatiles (H_2S, SO_2, HCl, HF, and NO_x) in the CO_2-rich sample (magmatic) and the presence of H_2S in the CO_2-poor (atmospheric) sample probably reflect the complex internal structure of the hydrothermal system as well as the differential solubility of H_2S and CO in hydrothermal solutions. Theoretical data and empirical studies of gases in geothermal fields have documented the wide ranges in CO_2/H_2S that can be produced in fumaroles by boiling and condensation cycles (Giggenbach, 1980). A better understanding of the internal structure of the hydrothermal system based on time integrated gas studies could led to determination of the extent to which alteration is presently occurring in the volcanic edifice. This information in turn would lead to better estimates of volcano edifice collapse probabilities contributing to a more complete hazard assessment.

8. Chemistry of fumarole condensates

Concentration data for the fumarole condensates and melt waters in the ice caves are summarized in Table 3. As might be expected, the melt water is essential pure with very low element concentrations. The condensates are also very dilute, although element enrichments are evident in both fumaroles, especially the upper one. The upper fumarole is slightly acidic, enriched in K and Na to ppm levels, enriched in metals such as Al, Pb, Zn Fe and Mn to ppb levels, and enriched in volatiles such as Cl, S, and F to ppb levels. The upper fumarole has the larger concentrations of metals consistent with the carbon

isotope and CO_2-rich gas composition which indicate that the upper fumarole had the greatest contribution of magmatic gases. However, the element concentrations are much lower than those in the high temperature fumaroles that formed after eruption of Mount St. Helens (Symonds and Reed, 1993) and which were derived both from degassing of magma and rock aerosols entrained in the gas stream. These low element concentrations probably reflect the enormous dilution that occurs when magmatic gases condense in the meteoric water reservoirs in the edifice of the volcano.

9. Mineralogy of vent incrustations

X-ray diffraction analyses of white, 1–2 mm incrustations along fractures of andesite at an inactive fumarole inside of the east crater ice cave revealed the presence of minor kaolin group clays, silica, and abundant sulfates and phosphates, including small amounts of natroalunite, minamiite, and woodhouseite. These minerals are consistent with the element enrichments noted in the condensate samples (Table 3) and include a similar assemblage to alteration minerals from the east crater rim, outside the caves, where kaolin, silica, gibbsite, and Ca–, Na–, K–, and Al–sulfates occur (Zimbelman, 1996). Minamiite and woodhouseite are alunite analog acid sulfate minerals that require the oxidation of H_2S and or the disproportionation of SO_2 for formation. Previous sulfur isotope analyses of alunite in altered rock on the summit of Mount Rainier indicate a strong component of magmatic hydrothermal alteration characterized by the disproportionation of magmatic SO_2 (Zimbelman, 1996; Zimbelman and Rye, 1996). Woodhouseite has been recognized in the magmatic hydrothermal alteration at Summitville, CO (Stoffregen and Alpers, 1987; Rye et al., 1992). Until more samples of the incrustations around fumaroles can be obtained and sulfur isotope compositions measured the possibility of magmatic SO_2 gases in recent fumaroles on Mount Rainier cannot be assessed (Rye et al., 1992). The incrustations are a minor feature of the ice caves, nevertheless their presence indicates that during the last 2000 years potentially dangerous pulses of sulfur-rich magmatic gases may have occurred.

Table 3
Chemistry of fumarole condensates[a]

Sample	pH	Spec cond (µg/l)	As (µg/l)	Sb (µg/l)	W (µg/l)	Mo (µg/l)	Fe (µg/l)	Mn (µg/l)	Ge (µg/l)	Ca (µg/l)	Mg (mg/l)	K (mg/l)	Na (mg/l)	Cl (mg/l)	SO$_4$ (mg/l)	NO$_3$ (mg/l)	F (mg/l)	SiO$_2$ (mµg/l)	Al (µg/l)
Lower fumarole	5.40	3	< 0.2	0.10	0.50	0.10	< 10	0.74	< 0.02	< 0.10	< 0.01	0.07	0.14	0.13	< 0.2	< 0.1	0.12	< 1	51
Upper fumarole	4.60	21	< 0.2	0.05	< 0.02	0.10	34	5.40	0.10	0.10	0.02	1.00	1.30	4.60	0.80	< 0.1	0.13	< 1	300
Melt water	5.40	2	< 0.2	0.05	4.20	0.06	< 10	0.41	< 0.02	< 0.10	< 0.01	0.03	0.06	< 0.1	0.70	< 0.1	< 0.1	< 1	2
Melt water	5.40	2	< 0.2	0.03	0.40	0.04	< 10	0.32	< 0.02	< 0.10	< 0.01	0.03	0.06	< 0.1	0.70	< 0.1	< 0.1	< 1	2

Sample	Pb (µg/l)	Zn (µg/l)	Cu (µg/l)	Co (µg/l)	Ni (µg/l)	Cr (µg/l)	Ti (µg/l)	V (µg/l)	Ag (µg/l)	Cd (µg/l)	Tl (µg/l)	Se (µg/l)	Ba (µg/l)	Cs (µg/l)	Li (µg/l)	Rb (µg/l)	Th (µg/l)	U (µg/l)	Sr (µg/l)
Lower fumarole	< 0.05	4	< 0.5	0.03	1.20	< 0.5	< 0.1	< 0.1	0.08	0.06	< 0.05	< 0.2	3.00	< 0.01	0.20	0.08	< 0.005	< 0.005	0.70
Upper fumarole	91.00	59	0.60	0.10	2.50	< 0.5	< 0.1	< 0.1	0.06	21.00	7.40	< 0.2	53.00	28.00	1.70	32.00	< 0.005	< 0.005	8.00
Melt water	< 0.05	3	< 0.5	0.02	0.30	< 0.5	< 0.1	< 0.1	0.02	0.03	0.07	< 0.2	0.40	< 0.01	< 0.1	0.04	< 0.005	< 0.005	0.30
Melt water	< 0.05	2	< 0.5	< 0.02	0.30	< 0.5	< 0.1	< 0.1	0.02	< 0.02	< 0.05	< 0.2	0.30	< 0.01	< 0.1	0.03	< 0.005	< 0.005	0.30

Sample	Re (µg/l)	Be (µg/l)	P (µg/l)	Y (µg/l)	La (µg/l)	Ce (µg/l)	Pr (µg/l)	Nd (µg/l)	Sm (µg/l)	Eu (µg/l)	Tb (µg/l)	Gd (µg/l)	Dy (µg/l)	Ho (µg/l)	Er (µg/l)	Tm (µg/l)	Yb (µg/l)	Hf (µg/l)	Ta (µg/l)
Lower fumarole	< 0.02	< 0.05	34	< 0.01	< 0.01	0.01	< 0.01	< 0.01	< 0.01	< 0.005	< 0.005	< 0.005	< 0.005	< 0.005	< 0.005	< 0.005	< 0.01	< 0.05	< 0.02
Upper fumarole	0.72	< 0.05	19	0.30	0.10	0.20	0.02	0.08	< 0.01	0.007	0.005	0.030	0.020	0.005	0.020	0.005	0.04	< 0.05	< 0.02
Melt water	< 0.02	< 0.05	5	< 0.01	< 0.01	< 0.01	< 0.01	< 0.01	< 0.01	< 0.005	< 0.005	< 0.005	< 0.005	< 0.005	< 0.005	< 0.005	< 0.01	< 0.05	< 0.02
Melt water	< 0.02	< 0.05	< 1	< 0.01	< 0.01	< 0.01	< 0.01	< 0.01	< 0.01	< 0.005	< 0.005	< 0.005	< 0.005	< 0.005	< 0.005	< 0.005	< 0.01	< 0.05	< 0.02

[a] pH and Spec cond (Specific Conductance) measurements made by David Grimes; NO$_3$, SO$_4$, F and Cl determinations made by Pete Theodorakos (Ion Chromatography); all other determinations made by Al Meier (ICP-Mass Spec).

10. Conclusions

Magmatic gases are the ultimate cause of the alteration that leads to large edifice collapse and potentially catastrophic debris flows on Mount Rainier and the critical issue for hazard assessment is to determine the location and the extent to which alteration is presently occurring within the volcano's edifice. The large mantle of glacial ice and the high heat flow leads to saturation of the edifice of the volcano by a meteoric water hydrothermal system that serves to condense magmatic gases. The history of magmatic gas flux on the summit of Mount Rainier is not well known. Clearly, magmatic degassing has occurred during the past 2000 years as indicated by the mineralogy of incrustations around now dormant fumarole vents. Further sulfur isotope work is needed on these incrustations to determine if magmatic gasses during the last 2000 years contained SO_2 as did the magmatic gases responsible for older summit alteration. The current magmatic system appears to be flooded by the extensive meteoric water hydrothermal system that probably consists of a series of stacked mixing, boiling, and condensation reservoirs.

Combining chemical and isotopic data has proven to be a powerful tool for understanding the details of hydrothermal systems including those in active stratovolcanoes (e.g. Landis and Rye, 1989; Arehart et al., 1995). An improved understanding of alteration processes within the volcanic edifice could be obtained from monitoring the temporal variations in both gas chemistry and isotopic compositions of the fumaroles. When coupled with seismic data this information could be used to evaluate the location of alteration currently occurring inside the volcano. For example, pulses of CO_2 are discharged through the summit fumaroles as different reservoirs become supersaturated and pressure on the hydrothermal system fluctuates. The magnitude of the changes in pressure on the system could be determined from monitoring maximum CO_2 concentrations over time, and this data when combined with seismic monitoring could identify possible sites of acid rock alteration.

The pattern of magmatic gas release on Mount Rainier is a concern for another reason. Episodic release of magmatic volatiles at otherwise dormant volcanoes presents a substantial risk for humans that frequent vent areas, as documented by numerous tragedies (Sigurdsson et al., 1987; Sigvaldason, 1989). For example, thermal activity near Crater Rock at Mount Hood displays many similar attributes to the summit thermal areas at Mount Rainier. Mount Hood volcano is host to areas of heated ground and fumaroles with near-boiling-point temperatures, acid-sulfate alteration mineralogy, and seasonal ice caves (e.g. Swanson et al., 1989; Zimbelman, 1996). In 1934, these ice caves were the site of a volcanic gas tragedy when a climber suffocated in oxygen-poor gas (Swanson et al., 1989). The summit caves at Mount Rainier have been used by climbers, in many cases as bivouacs during inclement weather, since the first documented summit climb (Stevens, 1876). While normally safe, these caves may present rapidly changing conditions, as indicated by results from fumarole measurements in this study and by real-time monitoring information from other volcanoes, such as nearby Mount St. Helens (e.g. McGee and Sutton, 1994; Harris and Rose, 1996). As with any active volcano, the risk of asphyxiation and carbon dioxide poisoning needs to be determined in the ice caves at Mount Rainier.

References

Arehart, G.B., Sturchio, N.C., Fischer, T.P., Williams, S.N., 1995. Gas chemistry and isotopic signature of fumaroles at Galeras Volcano, Colombia. PACRIM'95, pp. 19–28.

Coombs, H.A., 1936. The geology of Mount Rainier National Park. Geology 3, 131–212.

Crandell, D.R., 1963. Paradise debris flow at Mount Rainier, Washington. U.S. Geol. Surv. Prof. Pap. 475-B, B135–B139.

Crandell, D.R., 1971. Postglacial lahars from Mount Rainier Volcano, Washington. U.S. Geol. Surv. Prof. Pap. 677.

Crandell, D.R., 1976. The geologic story of Mount Rainier, Washington. U.S. Geol. Surv. Bull. 1292.

Crandell, D.R., Mullineaux, D.R., 1967. Volcanic hazards at Mount Rainier, Washington. U.S. Geol. Surv. Bull. 1238.

Crowley, J.K., Zimbelman, D.R., 1997. Mapping hydrothermally altered rocks on Mount Rainier, Washington, with Airborne Visible/Infrared Imaging Spectrometer (AVIRIS) data. Geology 25, 559–562.

Dansgaard, W., 1964. Stable isotopes in precipitation. Tellus 16, 436–468.

Deutsch, S., Ambach, W., Eisner, H., 1966. Oxygen isotope study of snow and firn on an alpine glacier. Earth Planet. Sci. Lett. 1, 197–201.

Dragovich, J.D., Pringle, P.T., Walsh, T.J., 1994. Extent and geometry of the Mid-Holocene Osceola Mudflow in the Puget Lowland—implications for Holocene sedimentation and paleogeography. Geology 22 (3), 3–26.

Driedger, C.L., Kennard, P.M., 1986. Ice volumes on Cascade volcanoes—Mount Rainier, Mount Hood, Three Sisters, and Mount Shasta, Washington. U.S. Geol. Surv. Prof. Pap. 1365.

Evans, W.C., Banks, N.G., White, L.D., 1981. Analyses of gas samples from the summit crater. In: Lipman, P.W., Mullineaux, D.R. (Eds.), The 1980 Eruptions of Mount St. Helens. U.S. Geol. Surv. Prof. Pap. 1250, pp. 227–231.

Faure, G., 1986. Principles of Isotope Geology, 2. Wiley, New York.

Fiske, R.S., Hopson, C.A., Waters, A.C., 1963. Geology of Mount Rainier National Park, Washington. U.S. Geol. Surv. Prof. Pap. 444.

Flett, J.B., 1912. The thermal caves (of Mount Rainier). The Mountaineer 5, 58–60.

Frank, D.G., 1985. Hydrothermal processes at Mount Rainier, Washington. PhD Thesis, University of Washington, Seattle, unpublished.

Frank, D., 1995. Surficial extent and conceptional model of hydrothermal system at Mount Rainier, Washington. J. Volcanol. Geotherm. Res. 65, 51–80.

Frank, D., Realmuto, V.J., 1995. Leakage from the active hydrothermal system at Mount Rainier, Washington. Eos, Am. Geophys. Union F644.

Giggenbach, W.F., 1980. Geothermal gas equilibria. Geochim. Cosmochim. Acta 44, 2021–2032.

Giggenbach, W.F., Stewart, M.K., 1982. Processes controlling the isotopic composition of steam and water discharges from steam vents and steam heated pools in geothermal areas. Geothermics 11, 71–80.

Grootes, P.M., Mook, W.G., Vogel, J.C., 1969. Isotopic fractionation between gaseous and condensed carbon dioxide. Zeitschr. Physik 221, 257–273.

Harris, D.M., Rose, W.I., 1996. Dynamics of carbon dioxide emissions, crystallization, and magma ascent: hypothesis, theory and applications to volcano monitoring at Mount St. Helens. Bull. Volcanol. 58, 163–174.

Hoblitt, R.P., Walder, J.S., Driedger, C.L., Scott, K.M., Pringle, P.T., Vallance, J.W., 1995. Volcano hazards from Mount Rainier, Washington. U.S. Geol. Surv. Open-File Rep. 95-273, 10 pp.

Javoy, M., Pineaum, F., Delorme, H., 1986. Carbon and nitrogen isotopes in the mantle. Chem. Geol. 57, 41–62.

Kiver, E.P., Mumma, M.D., 1971. Summit firn caves, Mount Rainier, Washington. Science 173, 320–322.

Kiver, E.P., Steele, W.K., 1972. Summit firn cave research, August 1971, Mount Rainier National Park, Washington. Geol. Soc. Am., Abstracts with Program, 4: 385.

Kiver, E.P., Steele, W.K., 1975. Firn caves in the volcanic craters of Mount Rainier, Washington. National Spel. Soc. Bull. 37, 45–55.

Kusakabe, M., 1997. Hazardous crater lakes. In: Scarpa, T., Tilling, R.I. (Eds.), Monitoring and Mitigation of Volcano Hazards. Springer, Berlin, pp. 573–598.

Landis, G.P., Rye, R.O., 1989. Reconnaissance gas chemistry of the Creede, Colorado, hydrothermal system. U.S. Geol. Surv. Open File Rep. 89-84, 51 pp.

Landis, G.P., Hofstra, A.H., 1991. Fluid inclusion gas chemistry as a potential minerals exploration tool: case studies from Creede, CO, Jerritt Canyon, NV, Coeur d'Alene district, ID and MT, Southern Alaska mesothermal veins, and mid-continent MVT's. J. Geochem. Explor. 42, 25–59.

Landis, G.P., Fitzpatrick, J.J., Everett, T., 1995. Analysis of firn gases collected at shallow depths in the Wrangell–St. Elias range, Alaska, the GISP2 site, Greenland, and the Taylor Dome site, East Antartica. U.S. Geol. Surv. Open-File Rep. 95-222.

Lange, I.M., Avent, J.C., 1975. Ground-based thermal infrared surveys of Mount Rainier volcano, Washington. Bull. Volcanol. 38, 929–943.

Lokey, W.M., 1973. Crater studies at a sleeping volcano. Explorers J. 51, 167–170.

Lokey, W., Rack, R., Miller, M.M., Prather, B.W., Kiver, E.P., 1972. Project Crater: Mt. Rainier glacio-volcanological research. Abstract, Arctic and Mountain Environments Symposium, Mich. St. Univ., Lansing.

Lopez, D.L., Williams, S.N., 1993. Catastrophic volcanic collapse: relation to hydrothermal processes. Science 260, 1794–1796.

Mariner, R.H., Presser, T.S., Evans, W.C., 1993. Geothermometry and water–rock interaction in selected thermal systems in the Cascade Range and Modoc Plateau, western United States. Geothermics 22, 1–15.

Matthes, F.E., 1914. Mount Rainier and its Glaciers. National Park Service: 1-48.

McGee, K.A., Sutton, A.J., 1994. Eruptive activity at Mount St. Helens, Washington, USA, 1984–1988: a gas geochemistry perspective. Bull. Volcanol. 56, 435–446.

Miller, M.M., 1970. Wind, sky, and ice. Explorers J. 48, 192–197.

Moran, E.M., Malone, S.D., 1997. Constraints on volcanic processes beneath Mount Rainier, Washington, From Local Earthquake Tomography. Eos, Trans., AGU. 78: F793.

Moran, S.C., Qamar, A., Malone, S.D., 1995. Seismicity at Mount Rainier, Washington. IUGG, XXI Gen. Assem. Abstracts: A453.

Moxham, R.M., Crandell, D.R., Marlatt, W.E., 1965. Thermal features at Mount Rainier, Washington, as revealed by infrared surveys. U.S. Geol. Surv. Prof. Pap. 525-D: 93-100.

National Research Council, 1994. Mount Rainier, active cascade

volcano-research strategies for mitigating risk from a high, snow-clad volcano in a populous region. National Academy Press.

Nehring, N.L., Mariner, R.H., White, L.D., Huebner, M.A., Roberts, E.D., Harmon, Karen, Bowen, P.A., Tanner, Lane, 1979. Sulfate thermometry of thermal waters in the western United States. U.S. Geol. Surv. Open-File Rep. 79-1135.

O'Neil, J.R., Friedman, I., 1977. Compilation of stable isotope fractionation factors of geochemical interest, Data of Geochemistry, 6th edition. U.S. Geol. Surv. Prof. Pap. 440-KK.

Riddihough, R., 1984. Recent movements of the Juan de Fuca plate system. J. Geophys. Res. 89, 6980–6994.

Russel, I.C., 1898. Glaciers of Mount Rainier. U.S. Geol. Surv. Annu. Rep. 18, 349–415.

Rye, R.O., 1993. SEG distinguished lecture: the evolution of magmatic fluids in the epithermal environment: the stable isotope perspective. Econ. Geol. 88, 733–753.

Rye, R.O., Bethke, P.M., Wasserman, M.D., 1989. Diverse origins of alunite and acid sulfate alteration: Stable isotope systematics. U.S. Geol. Surv. Open-File Rep. 89-5, 33 pp.

Rye, R.O., Bethke, P.M., Wasserman, M.D., 1992. The stable isotope geochemistry of acid sulfate alteration. Econ. Geol. 87, 225–262.

Scott, K.M., Vallance, J.W., Pringle, P.T., 1995. Sedimentology, behavior, and hazards of debris flows at Mount Rainier, Washington. U.S. Geol. Surv. Prof. Pap. 1547, 56 pp.

Sharp, R.P., Epstein, S., Vidziunas, 1960. Oxygen-isotope ratios in the Blue glacier, Olympic Mountains, Washington, USA. J. Geophys. Res. 65, 4043–4060.

Sherrod, D.R., Smith, J.G., 1990. Quaternary extrusion rates of the Cascade Range, northwestern United States and southern British Columbia. J. Geophys. Res. 95, 19,465–19,474.

Sigurdsson, H., Devine, J.D., Tchoua, F.M., Presser, T.S., Pringle, M.K.W., Evans, W.C., 1987. Origin of the lethal gas burst from Lake Monoun, Cameroon. J. Volcanol. Geotherm. Res. 31, 1–16.

Sigvaldason, G.E., 1987. International conference on Lake Nyos disaster, Yaound, Cameroon 16–20 March, 1987: conclusions and recommendations. J. Volcanol. Geotherm. Res. 39, 97–107.

Stevens, H., 1876. The ascent of Takhoma. Atlantic Monthly 38, 513–530.

Stoffregen, R.E., 1993. Stability relations of jarosite and natrojarosite at 100–250°C. Geochim. Cosmochim. Acta 58, 903–916.

Stoffregen, R.E., Alpers, C.N., 1987. Woodhouseite and svanbergite in hydrothermal ore deposits: products of apatite destruction during advanced argillic alteration. Can. Mineral. 25, 201–211.

Swanson, D.A., Cameron, K.A., Evarts, R.C., Pringle, P.T., Vance, J.A., 1989. IGC Field Trip Guidebook T106. AGU.

Symonds, R.B., Reed, M.H., 1993. Calculation of multicomponent chemical equilibria in gas–solid–liquid systems: calculation methods, thermochemical data, and applications to studies of high-temperature volcanic gases with examples from Mount St. Helens. Am. J. Sci. 293, 758–864.

Truesdell, A.H., Nathenson, M., Rye, R.O., 1977. The effects of subsurface boiling and dilution on the isotopic compositions of Yellowstone thermal waters. J. Geophys. Res. 82, 3694–3704.

Venezky, D.Y., Rutherford, M.J., 1997. Preeruption conditions and timing of dacite–andesite magma mixing in the 2.2 ka eruption at Mount Rainier. J. Geophys. Res. 102, 20,069–20,085.

Yamaguchi, D.K., 1983. New tree-ring dates for recent eruptions of Mount St. Helens. Quat. Res. 20, 246–250.

Zimbelman, D.R., 1996. Hydrothermal alteration and its influence on volcanic hazards—Mount Rainier, Washington, a Case History. PhD Thesis, University of Colorado, Boulder, unpublished.

Zimbelman, D.R., Rye, R.O., 1996. Dynamics of hydrothermal systems in an active stratovolcano—Mount Rainier, Washington. Geol. Soc. Am. Abstracts with Program, 28.